RESEARCH PAPER

Enzyme-encapsulated silica nanoparticle for cancer chemotherapy

Yi-Rong Chiu · Wei-Jen Ho · Jiun-Shuan Chao · Chiun-Jye Yuan

Abstract A novel horseradish peroxidase-encapsulated silica nanoparticle (SNP) was generated in this study under relatively mild conditions. The generated enzyme-encapsulated SNP were relatively uniform in size (average 70 ± 14.3 nm), monodispersed, and spherical, as characterized by transmission electron microscopy and scanning electron microscopy. The horseradish peroxidase encapsulated in silica nanoparticle exhibits biological properties, such as a pH-dependent activity profile and k_m value, similar to that of free enzymes. Furthermore, enzyme-encapsulated SNP exhibited good operational stability for the repetitive usage with a relative standard deviation of 5.1 % ($n = 10$) and a high stability for long term storage (>60 days) at 4 °C. The feasibility of using enzyme-encapsulated SNP in prodrug cancer therapy was also demonstrated by its capability to convert the prodrug indole-3-acetic acid into cytotoxic peroxyl radicals and trigger the death of tumor cells. These results indicate that the developed enzyme-encapsulated SNP has potential in the applications of prodrug cancer therapy.

Introduction

Nanotechnology is defined as the science and technology that design, synthesize, and characterize materials and devices at dimensions of nanometer scale. Human health care may be benefited by integrating both nanotechnology and biomedicine to improve the properties of already available therapeutic and diagnostic modalities, such as lowering doses of drug and increasing the therapeutic efficacy. Nanotechnology is also emerging as a promising tool to improve the diagnostic protocol, generate imaging agents, and synthesize and deliver drugs for detecting and treating cancers (Alexis et al. 2008; Bae et al. 2011; Farokhzad and Langer 2006; Ferrari 2005; Hock et al. 2011). Cancer is a devastating disease whereby cells grow out of control and invade neighboring tissues to cause acute illness and even death. Current conventional approaches, including surgery, chemotherapy, radiation

Y.-R. Chiu · W.-J. Ho · J.-S. Chao · C.-J. Yuan (✉)
Department of Biological Science and Technology, National Chiao Tung University, Hsinchu 300, Taiwan, ROC
e-mail: cjyuan@mail.nctu.edu.tw

C.-J. Yuan
Institute of Molecular Medicine and Bioengineering, National Chiao Tung University, Hsinchu 300, Taiwan, ROC

therapy, and immunotherapy, have been demonstrated to be effective for various cancers. However, normal tissues and cells may be damaged by the cytotoxic chemicals in chemotherapy and ionic radiation in radiation therapy, resulting in severe side effects. An increased system risk and local infection may also occur in immunotherapy and surgical removal of tumors. These disadvantages limit the application of these approaches in cancer treatment.

Enzyme–prodrug therapy (EPT) is a strategy whereby an exogenous enzyme is specifically targeted to tumor tissues by conjugated antibodies or other targeting molecules (Bagshawe 1990; Connors 1995). The targeted exogenous enzyme then specifically converts the nontoxic prodrug into the toxic drug that kills tumor cells. EPT not only provides a high selectivity for anticancer prodrug by enzyme catalysis, but also avoids the side-effects from chemotherapy, radiation therapy, or immunotherapy (Connors and Knox 1995; Gesson et al. 1994; Mauger et al. 1994). Several studies have focused on the delivery efficiency and the efficacy of the EPT system by conjugating enzymes on the surface of different nanomaterials, such as liposome (Huysmans et al. 2005), polymers (Ahmad et al. 2006; Kratz et al. 2006), dendrimer (Fuchs et al. 2004; Gopin et al. 2006), super paramagnetic iron oxide nanoparticles (SPION) (Petri-Fink et al. 2005), and silica beads (Guthaus et al. 2002; Rudolphi et al. 1995). However, low enzymatic recovery (Han and Amidon 2000; Harikrishna et al. 2003) and immunogenicity upon exposure of exogenous enzymes (Nishi 2003; Syrigos and Epenetos 1999) can occur with these methods and remains unsolved, hence limiting its applications in cancer therapy.

One of the possible solutions for the above problem is to shield the epitopes of exogenous enzymes by encapsulating them in porous organic or inorganic matrices. Enzyme immobilization by encapsulation plays important roles in enhancing protein stability, facilitating the separation of enzyme and reaction products, allowing multiple or repetitive usage of enzymes, and in establishing a multi-enzyme system for various industrial applications (Amine et al. 2006; Wu et al. 1994). Enzyme encapsulation in a porous organic or inorganic matrix has been utilized broadly to immobilize and stabilize fragile enzymes (Ho et al. 2006; Li et al. 2000). The integration of nanotechnology and enzyme immobilization exhibits several

advantages, including high loading capacity, large surface-to-volume ratio, and easy penetration of the plasma membrane (Baroli et al. 2007). These increase the efficacy of therapy and reduce side effects of therapeutic agents. The development of silica-based, enzyme-encapsulated nanoparticle exhibits several advantages, such as enzyme easily retain in the matrix network, provide good accessibility retain enzyme a porous nanostructure, exhibiting high hydrophilicity, and biocompatibility to the human body. These make these materials suitable for various clinical and biomedical applications (Karlsson 1999; Kawanabe et al. 1991). Furthermore, with their well-defined silanol groups on the surface, the silica nanoparticles, offer endless possibilities for modifications (Qhobosheane et al. 2001; Wu and Narsimha 2008). Although immobilization of enzyme in the silica-polysaccharide hybrid nano-composites has been reported previously (Shchipunov et al. 2004), the formation of clumping and clustering of the enzyme-entrapped nano-composites blocks their application in the clinical therapeutic protocols. The quality and efficacy of the developed nano-composites as the biomedicines are highly dependent on the monodispersity and size distribution of these products.

In this study, an exogenous horseradish peroxidase (HRP) was entrapped in the silica-based nanoparticles using sol–gel technology. The generated HRP-encapsulated silica nanoparticles, SNP(HRP)s, were characterized by their biophysical and biological properties, repetitive usage, reproducibility, and long term storage. HRP was recently reported to convert a nontoxic pro-drug, indole-3 acetic acid (IAA), into cytotoxic peroxyl radicals that trigger cell death of the tumor cells (Kim et al. 2004; Wardman 2002). Thus, the capability of SNP(HRP)s in oxidizing IAA was also investigated. This study demonstrates that the developed enzyme-encapsulated silica nanoparticle (ESNP) has great potential in cancer therapy applications.

Experimental

Materials

2′-azino-bis(3-ethylbenzthiazolin-6-sulfonate) (ABTS), tetraethylorthosilicate (TEOS, 98 %), ammonium hydroxide (NH_4OH), polyethylene glycol (PEG, molecular

weight 6,000), indole-3-acetic acid (IAA), MTT (3-(4, 5-dimethyldiazol-2-yl)-2,5 diphenyl tetrazolium bromide), and horseradish peroxidase (HRP, 181 U/mg) were purchased from Sigma-Aldrich. All other reagents and chemicals were analytical grade.

Preparation of enzyme encapsulated silica nanoparticles

HRP stock solution (5.52 mg/mL) was prepared by dissolving HRP in 100 mM Tris–HCl buffer, pH 8.6. One unit of HRP is defined as oxidizing 1 μmol of ABTS per min at 25 °C and pH 5.0. Silica sol was prepared by mixing 0.56 mL of TEOS with water and ethanol to give a molar ratio of water:TEOS:ethanol = 200:1:160. The resulting mixture was then sonicated in an ultrasonic cleaner with the power and frequency of 150 W and 46 kHz, respectively, (UC-450, Enshine Scientific Co., Taiwan, ROC) at 22 °C for 15 min. HRP/TEOS sol mixture was prepared by adding 1 mL HRP stock solution in drops into the TEOS sol, followed by sonicating at 22 °C for 10 min. The HRP/TEOS sol mixture was then fed at a constant flow rate of 6 mL min^{-1} into a flask containing 10 M NH$_4$OH with sonication to generate SNP(HRP)s. After sonication for 30 min, 1 mL of 50 mM PEG was added into the SNP(HRP)s suspension at room temperature for 120 min for surface modification. SNP(HRP)s were collected by centrifuging at $16100 \times g$ and washed twice with PBS buffer (137 mM NaCl, 2.7 mM KCl, 10 mM Na$_2$HPO$_4$, 1.76 mM KH$_2$PO$_4$, pH 6.8) to remove residues of ammonia.

Nanoparticle characterization

The developed SNP(HRP)s were monitored under field emission scanning electron microscope (FE-SEM, S4700, HITACHI) and transmission electron microscope (FETEM, JEM-2100F, JEOL). The size distribution of the silica nanoparticles was measured by dynamic light scattering (LB-550, HORIBA).

Activity assay

The activity of free HRP or HRP-SNP was determined calorimetrically using ABTS and H$_2$O$_2$ as substrates. The activity assay was performed by mixing HRP (0.5 U) or SNP(HRP) suspension (0.5 U) into 1 mL of reaction solution (0 3 mM H$_2$O$_2$ and 0.5 mM ABTS in 100 mM sodium acetate buffer, pH 5.0) at room temperature for 1 min, followed by monitoring absorbance at 425 nm. Total volume of reaction solution is 1 mL.

HPLC analysis

The oxidation of IAA by free HRP (0.05 U) or SNP(HRP) (0.05 U) was carried out in a 100 mM sodium acetate buffer (pH 5.0) containing 500 μM IAA at 25 °C for 5 min. An aliquot of reaction mixture (200 μL) was analyzed by reverse-phase HPLC on a C$_{18}$ Columbus column (30 nm, 5 μm, 250 mm × 4.6 mm; GL Sciences, JAPAN) using an isocratic elution buffer of methanol/1 % acetic acid mixture (40:60, v/v) at a flow rate of 1.0 mL/min. The eluted products were monitored at absorbance of 250 nm using an Agilent 1100 series detector.

Cell culture

HeLa cells were cultured in Dulbecco's modified Eagle's medium (PAA Laboratories GmbH) containing 10 % fetal calf serum, 100 units/mL penicillin, and 100 μg/mL streptomycin (PAA Laboratories GmbH) in a 37 °C cultural chamber with 5 % CO$_2$.

Cell viability assay

HeLa cells (8×10^{-4} cells/well) were seeded in 24-well cultural plates at 37 °C and 5 % CO$_2$ for overnight or until it reached 70 % confluency. Cells collected before or after treatments were incubated with 0.5 mL MTT solution (0.5 mg/mL cultural medium) at 37 °C for 3 h. The formazan dye formed was made soluble by acid-isopropanol and the absorbance was measured at 570 nm.

Fluorescent microscopy

HeLa cells were washed twice with pre-warmed PBS and fixed with 1 mL 4 % paraformaldehyde in PBS at room temperature for 20 min. After fixation, the cells' membrane were penetrated by 0.01 % Triton X-100 at room temperature for 30 min. Cells were washed three times with PBST (137 mM NaCl, 2.7 mM KCl, 10 mM Na$_2$HPO$_4$, 2 mM KH$_2$PO$_4$, and 0.05 % Tween-20), followed by staining with 5 μg/mL

4′,6′-diamidino-2-phenylindole (DAPI) at room temperature for 20 min. After DAPI staining, cells were washed twice with PBST. The fluorescent images were monitored under a fluorescent microscope (Nikon Eclipse TE2000-U).

Results and discussion

Preparation of SNP(HRP)s

The generation of SNP(HRP)s was proposed to protect the exogenous HRP from degradation, to stabilize the structure of exogenous enzymes, and to reduce the immune responses of hosts in the application of the EPT-based cancer therapy. The porous property of silica nano-matrix allows the encapsulated enzymes to access the prodrug and release the toxic product easily (Fig. 1a). The therapeutic efficacy of the developed SNP(HRP)s in the application of EPT depends on several factors, including the size distribution, monodispersity, and the stability of enzymes encapsulated in the nano-composites. Therefore, the preparation of SNP(HRP)s was carried out using the mild sol–gel process. The spherical, monodispersed SNP(HRP)s could be successfully synthesized by adding the mixture of HRP/TEOS sol into 10 M NH$_4$OH at 0 °C with a feeding rate of 6 mL min^{-1} and a constant sonication (Supplementary Figure S1). Interestingly, the size of the prepared SNP(HRP)s was reverse proportional to the molar ratio of water to TEOS precursor (R value), and the concentration of NH$_4$OH used in the sol–gel process (Table 1 and Supplementary Figure S1). When the R value of TEOS sol increased from 50 to 1,000, the size of synthesized SNP(HRP)s changed from 83 ± 16 to 24 ± 1.0 nm in diameter (Table 1, Ex. 1 to Ex. 5). NH$_4$OH functions as a catalyst to promote both the hydrolysis and condensation of TEOS in ethanol. When SNP(HRP)s were synthesized under the R value of 200, the size of the nanoparticles increased with the decrease of the concentrations of NH$_4$OH (Table 1, Ex. 6 to Ex. 10). The size of the synthesized SNP(HRP)s was also affected by the feeding rate of HRP/TEOS sol mixture dropping into the ammonia. As shown in Table 1, the size of SNP(HRP)s decreased with increase of feeding rate (Ex. 3, Ex. 11 and Ex. 12). It has been suggested that the particle size and morphology of silica nanoparticles depend strongly on the hydrolysis

kinetics (Matsoukas and Gulari 1988; Park et al. 2002; Van Helden et al. 1981). Therefore, the formation of small SNP(HRP)s in this study may be facilitated by the fast hydrolysis of TEOS in sol with high R value and high concentration of NH$_4$OH.

The activity of encapsulated HRP in SNP(HRP)s was determined by chromametric method using ABTS and H$_2$O$_2$ as substrates (Table 1, Ex. 1 to Ex. 5). The result showed that the specific activity of the encapsulated HRP in SNP(HRP)s gradually increased from Ex. 1 to Ex. 4. Although the specific activity of entrapped HRP in Ex. 4 was the highest among the SNP(HRP)s tested, the nano-composites synthesized were not uniform (Supplementary Figure S1, Ex. 4). For this reason, the SNP(HRP)s of Ex. 3 were adopted for the rest experiments. The condition for the synthesis of Ex. 3 SNP(HRP)s was adding the mixture of HRP and TEOS sol (molar ratio of water:TEOS: ethanol = 200:1:160) into a flask containing 10 M NH$_4$OH under the room temperature with a feeding rate of 6 mL min^{-1}. The encapsulation of HRP in SNP was demonstrated by its ability to resist the depriving effect of stripping agents, such as 1 M NaCl and 0.1 % Tween-20 in phosphate buffer saline (Supplementary Figure S2, closed circle). In contrast, the HRP absorbed on the SNPs could be easily removed by the above treatment (Supplementary Figure S2, closed square). These results suggest that HRP is successively encapsulated in the silica nanoparticles without leakage.

Characterization of SNP(HRP)

The micrographic images of scanning electron microscopy (SEM) and transmission electron microscopy (TEM) show that the generated SNP(HRP)s are spherical and mono-dispersed with an average particle size of about 70 ± 14.3 nm (Fig. 1b, c). The calcium ion, which maintains the structural integrity of the HRP, was also detected in the developed SNP(HRP) by energy dispersive X-ray (EDX) analysis (Supplementary Figure S3), whereas the same signal was totally absent in SNP only. These results indicate that relatively uniform and mono-dispersed SNP(HRP) can be successfully generated under mild conditions.

The developed SNP(HRP)s were then further characterized by their pH dependency and ability for long term storage. The pH-dependency of peroxidase activity of SNP(HRP)s was determined in a pH range from 4.0 to 7.0 using 0.5 mM ABTS and 3 mM

Fig. 1 a The scheme illustrating the formation of SNP(HRP). Developed SNP(HRP) was imaged using SEM (**b**) and TEM (**c**). The magnification power is 5.0 kV. *Scale bar* in (**c**) is 50 nm
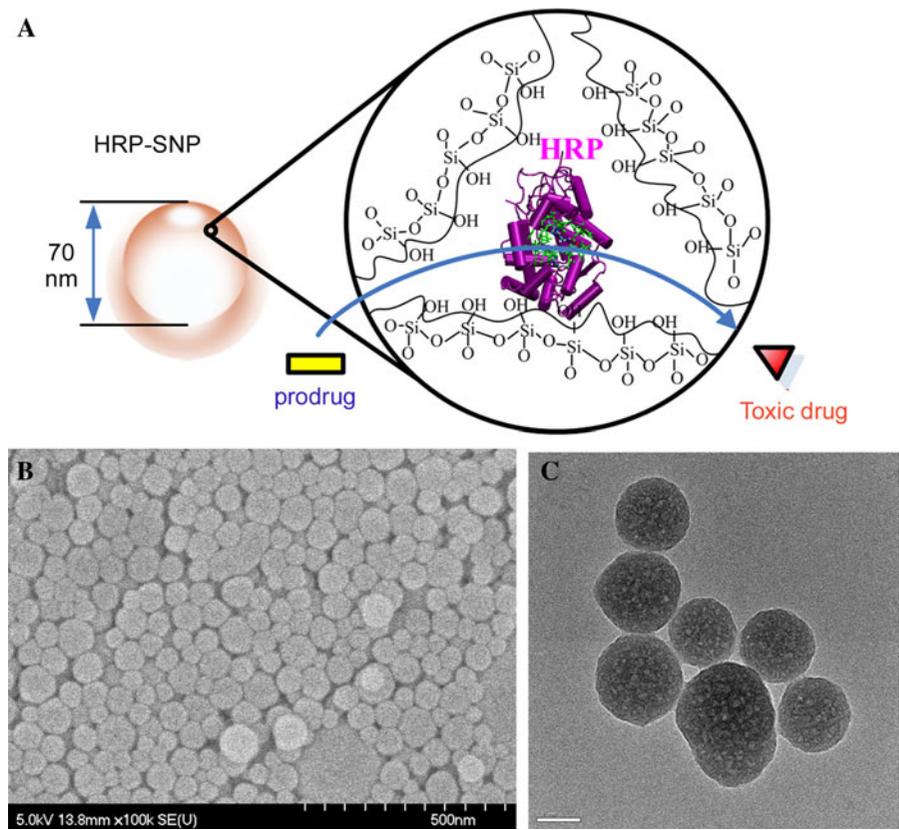

Table 1 The SNP(HRP)s were synthesized under fixed HRP (1,000 U) and different R value NH$_4$OH or feeding rate

Samples	Experimental conditions					Results
	R value	Ethanol	Feeding rate	NH$_4$OH	Activity of encapsulated HRP (mU/mg)[a]	Average particle size $\pm$ SD
	[H$_2$O]/[TEOS]	(M)	(mL/min)	(M)		(nm)
Ex. 1	50	4	6	10	6.37	83 $\pm$ 16
Ex. 2	100	4	6	10	7.02	77 $\pm$ 3
Ex. 3	200	4	6	10	7.29	70 $\pm$ 1.4
Ex. 4	500	4	6	10	7.51	36 $\pm$ 3
Ex. 5	1,000	4	6	10	3.92	24 $\pm$ 1
Ex. 6	200	4	6	8	–	134 $\pm$ 10
Ex. 7	200	4	6	6	–	188 $\pm$ 15
Ex. 8	200	4	6	4	–	270 $\pm$ 17
Ex. 9	200	4	6	2	–	386 $\pm$ 56
Ex. 10	200	4	6	1	–	534 $\pm$ 79
Ex. 11	200	4	3	10	–	94 $\pm$ 17
Ex. 12	200	4	1	10	–	217 $\pm$ 35

[a] mU of HRP per mg of nano-particles

hydrogen peroxide (H$_2$O$_2$) as substrates. As shown in Fig. 2a, the activity of SNP(HRP) increased when the pH was changed from 4.0 to 5.0, and then declined when the pH was 7.0 with a maximal activity at a pH of 5.0. This result shows that the encapsulated HRP exhibits a similar pH profile to that of free HRP
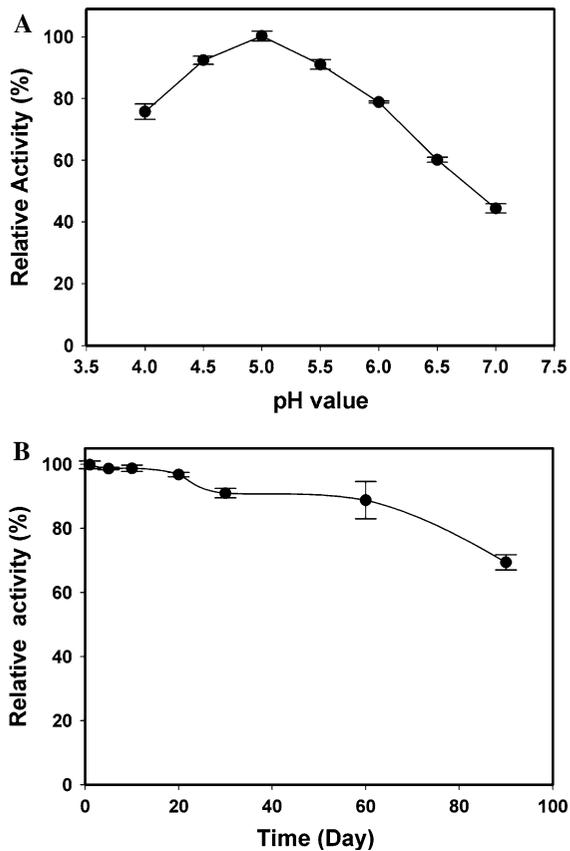
Fig. 2 The Characteristics of SNP(HRP). **a** The pH-dependence reaction profile of SNP(HRP). The peroxidase activity of SNP(HRP) was performed in a 100 mM sodium acetate buffer (pH 4.0 ∼ pH 5.5) or in a 100 mM sodium phosphate buffer (pH 6.0 ∼ 7.0) containing 0.5 mM ABTS and 3 mM H_2O_2. The reactions were performed at 25 °C for 1 min and the activity of SNP(HRP) was determined by monitoring absorbance at 405 nm. **b** The long-term stability of SNP(HRP) after storage at 4 °C. The SNP(HRP) was stored at 4 °C and assayed at indicated times to determine the remnant peroxidase activity. The results are represented as means ± S.D obtained from three independent experiments

(Gallati 1979). The biological property of encapsulated HRP was also investigated by kinetic analysis using ABTS and H_2O_2 as substrates. The k_m of encapsulated HRP to ABTS at pH 5.0 was 1.3 ± 0.14 mM, whereas, the k_m of free HRP to ABTS at pH 7.0 and 5.0 was 2.0 mM (Hiner et al. 1996) and 2.6 mM (Bauduin et al. 2006), respectively. These results indicate that the entrapped HRP exhibit similar kinetics to that of free HRP.

Stability of SNP(HRP)

Repetitive usage and long term stability of SNP(HRP) are essential for its future applications in various fields. At room temperature, the activity of SNP(HRP) was repetitively measured 13 times. About 85 % original activity of SNP(HRP) was retained after 10 reactions with a relative standard deviation (R.S.D) of 5.1 % (Supplementary Figure S4). However, about 80 % of original activity was retained even after 13 reactions. The oxidative inactivation by H_2O_2 (Rodriguez-López et al. 2000) and the incomplete recovery during the washing-drain cycles between reactions may explain the activity lost after repetitive activity measurement. These results demonstrate that the developed SNP(HRP) exhibits a capability for repetitive usage with good reproducibility.

The long term stability of SNP(HRP) was also determined by periodically determining the activity of encapsulated HRP after storing at 4 °C. Interestingly, more than 85 % of original peroxidase activity of SNP(HRP) was retained after two months (Fig. 2b). Even after 3 months, about 70 % of the original activity was preserved. These results reveal that proteins and enzymes can be stably entrapped in the silica matrix by the sol–gel procedure without losing much of their biological activity.

IAA-dependent cytotoxicity of SNP(HRP)

The application of HRP-SNP in EPT was initially investigated by oxidizing the nontoxic prodrug IAA into cytotoxic products (Kim et al. 2004; Wardman 2002). The oxidation of IAA catalyzed by free HRP and SNP(HRP) at pH 5.0 was analyzed by reverse phase high performance liquid chromatography (HPLC). The HPLC elution profiles showed that both free and encapsulated HRP could catalyze the oxidation of IAA and generate five similar oxidized products (peaks a–e) (Fig. 3, panels A and B; Supplementary Materials). These oxidized products could be partially identified by their ultraviolet absorption spectra (Candeias et al. 1996; Gazarian et al. 1998; Hinman and Lang 1965; Kobayashi et al. 1984; Smith et al. 1982) as oxindol-3-yl carbinol (peak a; peak absorption = 250 nm) (Kim et al. 2004), indol-3-yl methanol (peak b; peak absorption = 278 nm) (Candeias et al. 1996; Smith et al. 1982), indole-3-aldehyde (peak c; peak absorption = 240,
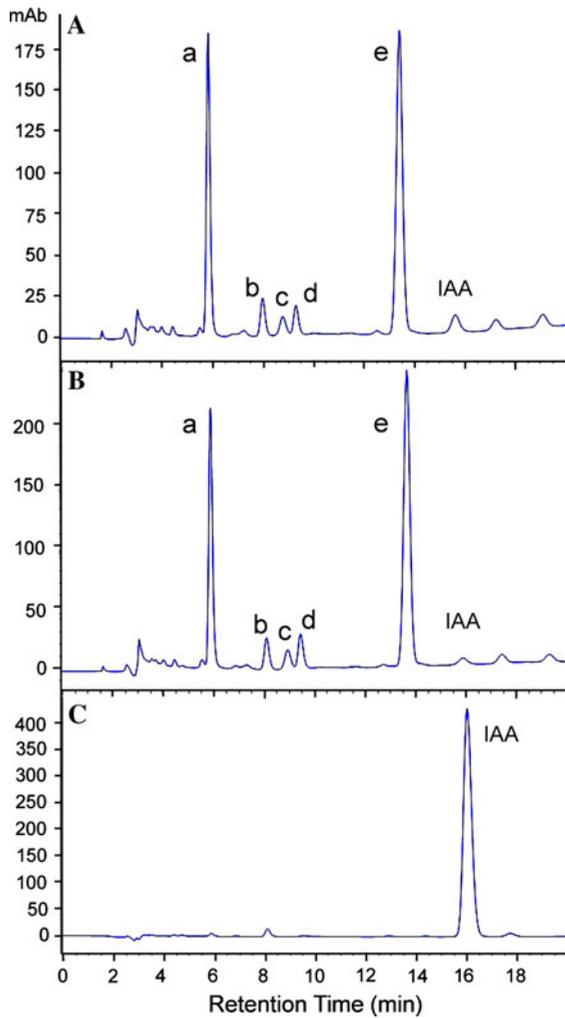
Fig. 3 Elution profiles of the oxidative products of IAA by free HRP or SNP(HRP)s. The oxidation of IAA (500 μM) by free HRP (**A**) or SNP(HRP)s (**B**) in 100 mM sodium acetate buffer, pH 5.0 was performed at room temperature for 5 min. The IAA alone was used as a standard (**C**). The reaction products were analyzed on the reverse-phase HPLC with a C$_{18}$ Columbus column. The eluted products were monitored at O.D. 250 nm

Fig. 4 Viability of HeLa cells before and after the treatment of SNP(HRP) and IAA. HeLa cells were incubated with mock (*filled circle*), 1.8 U HRP (*circle*), SNP (*square*), and 1.8 U SNP(HRP) (*filled inverted triangle*) in the presence of various concentrations of IAA (0 to 3.2 mM) at 37 °C for 6 (**a**) or 24 h (**b**). After incubation, the viability of the HeLa cells was determined by MTT assay. The results are represented as means ± S.D obtained from three independent experiments

300 nm) (Gazarian et al. 1998), sketolyl-hydroperoxide (peak d; peak absorption = 270, 278 nm) (Gazarian et al. 1998), and 3-methylene-oxindole (peak e; peak absorption = 253 nm) (Hinman and Lang 1965). The mass spectroscopy analysis of products b, c, and e further confirms the above results (Supplementary Figure S5). These results reveal that SNP(HRP) functions as the free HRP to convert IAA into oxidized products, suggesting its potential in the application of EPT.

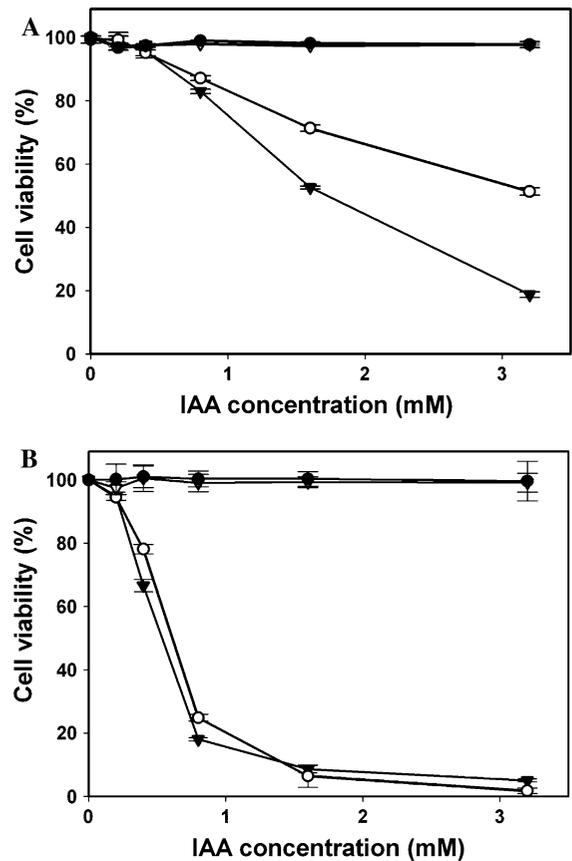The application of SNP(HRP) in the EPT was further explored using a HeLa cell, a human cervical tumor cell line, as a model. Accordingly, HeLa cells were incubated with various concentrations of IAA (0 to 3.2 mM) in the presence and absence of SNP(HRP) (1.8 U) at 37 °C for 6 h (Fig. 4a) or 24 h (Fig. 4b). Without IAA, silica nanoparticle (SNP) and SNP(HRP) were not toxic to HeLa cells even after incubation at 37 °C for more than 24 h (data not shown). HeLa cells were 100 % viable when incubated with IAA alone (Fig. 3, filled circle) or the combination of IAA and SNP (Fig. 3, square) at 37 °C for 6 or 24 h. However, in combination with SNP(HRP), (1.8 U) IAA became cytotoxic to HeLa cells (Fig. 3, filled inverted triangle), exhibiting a IC$_{50}$ of 1.72 mM and 0.53 mM for 6 and 24 h treatments, respectively. After treating with
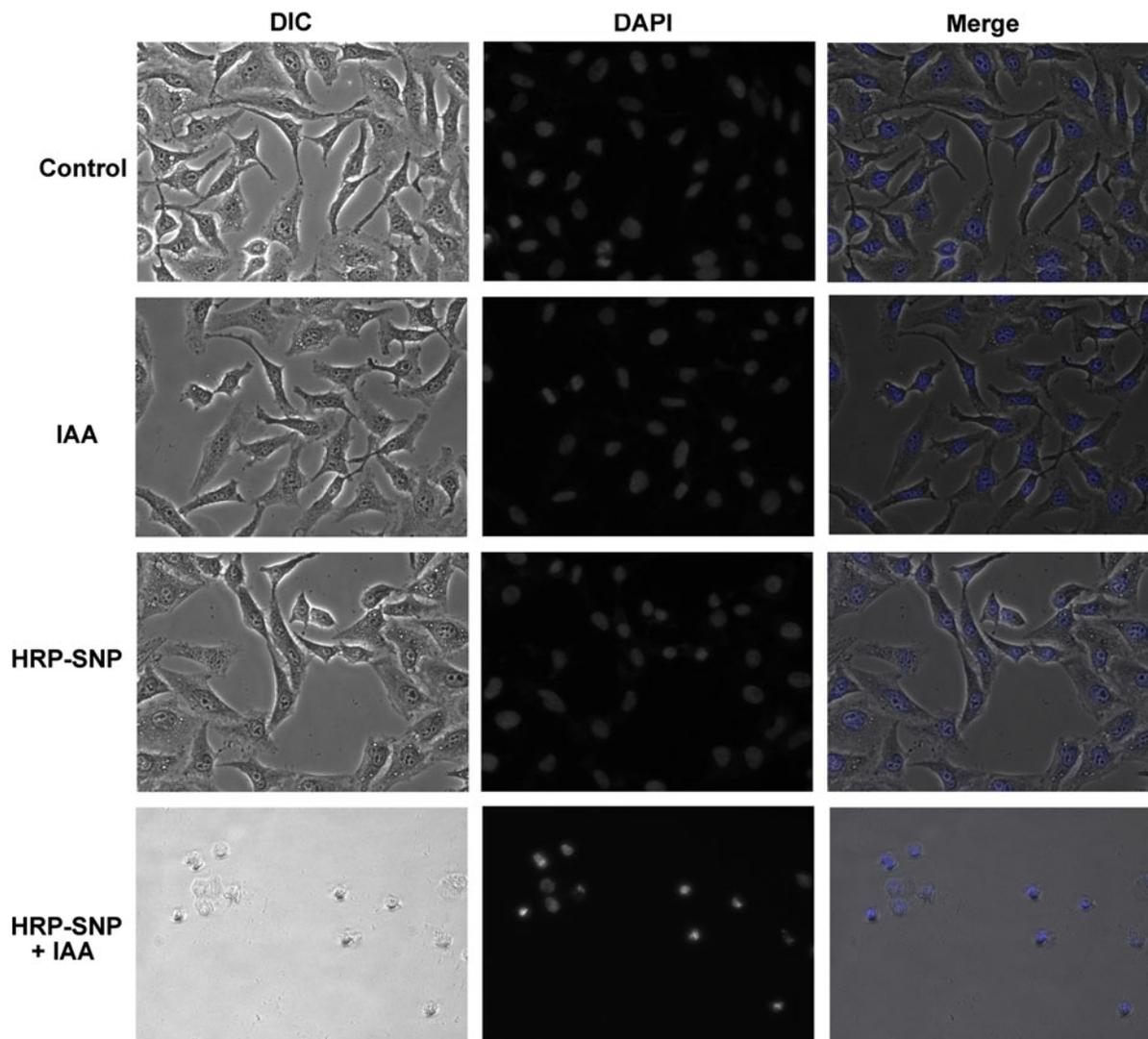
Fig. 5 Fluorescent images of HeLa cells after the treatment of SNP(HRP) and IAA. HeLa cells were treated without (HeLa) or with IAA (1.6 mM) (IAA), SNP(HRP) (1.8 U) (SNP(HRP)) and the combination of IAA (1.6 mM) and SNP(HRP) (1.8 U) (SNP(HRP) + IAA) at 37 °C for 18 h. Cells were fixed with 4 % paraformaldehyde, followed by staining with 5 µg/mL DAPI

0.8 mM IAA for 24 h, the viability of HeLa cells reduced by about 80 %, whereas, with 1.6 mM IAA, only about 5 % of HeLa cells were still viable after 24 h treatment. A similar result was also found in a treatment with the combination of free HRP and IAA. In the presence of free HRP (Fig. 4, circle), the IC$_{50}$ of IAA is around 3.2 mM and 0.61 mM for 6 and 24 h treatments, respectively.

The morphological change of the HeLa cells incubated with SNP(HRP) and IAA was also studied by light and fluorescent microscopes. HeLa cells treated with SNP(HRP) (1.8 U) and 0.8 mM IAA at 37 °C for 18 h exhibited nuclear condensation and a profound shrunken morphology (Fig. 5), suggesting the induction of apoptosis. No morphological changes were observed in cells treated with IAA alone or the combination of IAA and SNP. These results indicate that the fabricated SNP(HRP) has a potential to replace free HRP in enzyme–prodrug cancer therapy.

Conclusion

In this study, we have successfully developed a novel enzyme-encapsulated silica nanoparticle (ESNP) using a sol–gel process. The properties of the encapsulated HRP were relatively unchanged as demonstrated by its pH-dependent profile, kinetics and capability to oxidize IAA. The generated SNP(HRP) exhibits good reproducibility in repetitive enzyme activity measurements and long term stability. The feasibility of SNP(HRP) in the enzyme/prodrug cancer therapy was also demonstrated by converting the nontoxic prodrug IAA into the toxic radical products that trigger the cell death of HeLa cells. In conclusion, the developed ESNP exhibited several features that make it suitable for future cancer chemotherapy and a variety of biomedical applications.

References

Ahmad S, Tester RF, Corbett A, Karkalas J (2006) Dextran and 5-aminosalicylic acid (5-ASA) conjugates: synthesis, characterisation and enzymic hydrolysis. Carbohydr Res 341:2694–2701

Alexis F, Rhee JW, Richie JP, Radovic-Moreno AF, Langer R, Farokhzad OC (2008) New frontiers in nanotechnology for cancer treatment. Urol Oncol: Semin Ori Invest 26:74–85

Amine A, Mohammadi H, Bourais I, Palleschi G (2006) Enzyme inhibition-based biosensors for food safety and environmental monitoring. Biosens Bioelectron 21:1405–1423

Bae KH, Chung HJ, Park TG (2011) Nanomaterials for cancer therapy and imaging. Mol Cell 31:295–302

Bagshawe K (1990) Antibody-directed enzyme/prodrug therapy (ADEPT). Biochem Soc Trans 18:750–752

Baroli B, Ennas MG, Loffredo F, Isola M, Pinna R, López-Quintela MA (2007) Penetration of metallic nanoparticles in human full-thickness skin. J Invest Dermatol 127:1701–1712

Bauduin P, Nohmie F, Touraud D, Neueder R, Kunz W, Ninham BW (2006) Hofmeister specific-ion effects on enzyme activity and buffer pH: horseradish peroxidase in citrate buffer. J Mol Liq 123:14–19

Candeias LP, Folkes LK, Porssa M, Parrick J, Wardman P (1996) Rates of reaction of indoleacetic acids with horseradish peroxidase compound I and their dependence on the redox potentials. Biochemistry 35:102–108

Connors TA (1995) The choice of prodrugs for gene directed enzyme prodrug therapy of cancer. Gene Ther 2:702–709

Connors TA, Knox RJ (1995) Prodrugs in cancer chemotherapy. Stem Cells 13:501–511

Farokhzad OC, Langer R (2006) Nanomedicine: developing smarter therapeutic and diagnostic modalities. Adv Drug Deliv Rev 58:1456–1459

Ferrari M (2005) Cancer nanotechnology: opportunities and challenges. Nat Rev Cancer 5:161–171

Fuchs S, Kapp T, Otto H, Schoneberg T, Franke P, Gust R, Schlüter AD (2004) A set of surface-modified dendrimers with potential application as drug delivery vehicles: synthesis, in vitro cytotoxicity, and intracellular localization. Chemistry 10:1167–1192

Gallati H (1979) Horseradish peroxidase: a study of the kinetics and the determination of optimal reaction conditions, using hydrogen peroxide and 2,2′-azinobis 3-ethylbenzthiazoline-6-sulfonic acid (ABTS) as substrates. J Clin Chem Clin Biochem 17:1–7

Gazarian IG, Lagrimini LM, Mellon FA, Naldrett MJ, Ashby GA, Thorneley RN (1998) Identification of skatolyl hydroperoxide and its role in the peroxidase-catalysed oxidation of indol-3-yl acetic acid. Biochem J 333:223–232

Gesson JP, Jacquesy JC, Mondon M, Petit P, Renoux B, Andrianomenjanahary S, Van Dufat-Trinh H, Koch M et al (1994) Prodrugs of anthracyclines for chemotherapy via enzyme-monoclonal antibody conjugates. Anticancer Drug Des 9:409–423

Gopin A, Ebner S, Attali B, Shabat D (2006) Enzymatic activation of second-generation dendritic prodrugs: conjugation of self-immolative dendrimers with poly(ethylene glycol) via click chemistry. Bioconj Chem 17:1432–1440

Guthaus E, Burgle M, Schmiedeberg N, Hocke S, Eickler A, Kramer MD, Sweep CG, Magdolen V et al (2002) uPA-silica-particles (SP-uPA): a novel analytical system to investigate uPA–uPAR interaction and to test synthetic uPAR antagonists as potential cancer therapeutics. Biol Chem 383:207–216

Han HK, Amidon GL (2000) Targeted prodrug design to optimize drug delivery. AAPS PharmSci 2:E6

HariKrishna D, Rao AR, Krishna DR (2003) Selective activation of anthracycline prodrugs for use in conjunction with ADEPT. Drug News Perspect 16:309–318

Hiner ANP, Hernández-Ruíz J, Amao MB, García-Cánovas F, Acosta M (1996) A comparative study of the purity, enzyme activity, and inactivation by hydrogen peroxide of commercially available horseradish peroxidase isoenzymes A and C. Biotechnol Bioeng 50:655–662

Hinman RL, Lang J (1965) Peroxidase-catalyzed oxidation of indole-3-acetic acid. Biochemistry 4:144–158

Ho W-J, Yuan C-J, Reiko O (2006) Application of SiO$_2$-poly(dimethylsiloxane) hybrid material in the fabrication of amperometric biosensor. Anal Chim Acta 572:248–252

Hock SC, Ying YM, Wah CL (2011) A review of the current scientific and regulatory status of nanomedicines and the challenges ahead. PDA J Pharm Sci Technol 65:177–195

Huysmans G, Ranquin A, Wyns L, Steyaert J, Van Gelder P (2005) Encapsulation of therapeutic nucleoside hydrolase in functionalised nanocapsules. J Control Release 102:171–179

Karlsson KH (1999) Bone implants—a challenge to materials science. Ann Chir Gynaecol 88:226–235

Kawanabe K, Yamamuro T, Nakamura T, Kotani S (1991) Effects of injecting massive amounts of bioactive ceramics in mice. J Biomed Mater Res 25:117–1128

Kim DS, Jeon SE, Park KC (2004) Oxidation of indole-3-acetic acid by horseradish peroxidase induces apoptosis in G361 human melanoma cells. Cell Signal 16:81–88

Kobayashi S, Sugioka K, Nakano H, Nakano M, Tero-Kubota S (1984) Analysis of the stable end products and intermediates of oxidative decarboxylation of indole-3-acetic acid by horseradish peroxidase. Biochemistry 23:4589–4597

Kratz F, Warnecke A, Schmid B, Chung DE, Gitzel M (2006) Prodrugs of anthracyclines in cancer chemotherapy. Curr Med Chem 13:477–523

Li X, Zhang Y, Yan R, Jia W, Yuan M, Deng X, Huang Z (2000) Influence of process parameters on the protein stability encapsulated in poly-DL-lactide-poly(ethylene glycol) microspheres. J Control Release 68:41–52

Matsoukas T, Gulari E (1988) Dynamics of growth of silica particles from ammonia-catalyzed hydrolysis of tetra-ethyl-orthosilicate. J Colloid Interface Sci 124:252–261

Mauger AB, Burke PJ, Somani HH, Friedlos F, Knox RJ (1994) Self-immolative prodrugs: candidates for antibody-directed enzyme prodrug therapy in conjunction with a nitro-reductase enzyme. J Med Chem 37:3452–3458

Nishi Y (2003) Enzyme/abzyme prodrug activation systems: potential use in clinical oncology. Curr Pharm Des 9: 2113–2130

Park SK, Kim KD, Kim HT (2002) Preparation of silica nano-particles: determination of the optimal synthesis conditions for small and uniform particles. Colloids Surf A Physicochem Eng Aspects 197:7–17

Petri-Fink A, Chastellain M, Juillerat-Jeanneret L, Ferrari A, Hofmann H (2005) Development of functionalized super-paramagnetic iron oxide nanoparticles for interaction with human cancer cells. Biomaterials 26:2685–2694

Qhobosheane M, Santra S, Zhang P, Tan W (2001) Biochemically functionalized silica nanoparticles. Analyst 126: 1274–1278

Rodriguez-López JN, Gilabert MA, Tudela J, Thorneley RN, Garcia-Cánovas F (2000) Reactivity of horseradish per-oxidase compound II toward substrates: kinetic evidence for a two-step mechanism. Biochemistry 39:13201–13209

Rudolphi A, Vielhauer S, Boos KS, Seidel D, Bathge IM, Berger H (1995) Coupled-column liquid chromatographic analysis of epirubicin and metabolites in biological material and its application to optimization of liver cancer therapy. J Pharm Biomed Anal 13:615–623

Shchipunov YA, Karpenko TY, Bakunina IY, Burtseva YV, Zvyagintseva TN (2004) A new precursor for the immo-bilization of enzymes inside sol–gel-derived hybrid silica nanocomposites containing polysaccharides. J Biochem Biophys Methods 58:25–38

Smith AM, Morrison WL, Milham PJ (1982) Oxidation of indole-3-acetic acid by peroxidase: involvement of reduced peroxidase and compound III with superoxide as a product. Biochemistry 21:4414–4419

Syrigos KN, Epenetos AA (1999) Antibody directed enzyme prodrug therapy (ADEPT): a review of the experimental and clinical considerations. Anticancer Res 19:605–613

Van Helden AK, Jansen JW, Vrij A (1981) Preparation and characterization of spherical monodisperse silica disper-sions in nonaqueous solvents. J Colloid Interface Sci 81: 354–368

Wardman P (2002) Indole-3-acetic acids and horseradish per-oxidase: a new prodrug/enzyme combination for targeted cancer therapy. Curr Pharm Res 8:1363–1374

Wu X, Narsimha G (2008) Characterization of secondary and tertiary conformational changes of beta-lactoglobulin adsorbed on silica nanoparticle surfaces. Langmuir 24: 4989–4998

Wu S, Lin J, Chan SI (1994) Oxidation of dibenzothiophene catalyzed by heme-containing enzymes encapsulated in sol–gel glass. A new form of biocatalysts. Appl Biochem Biotechnol 47:11–20